Bulk and surface oxygen vacancy formation and diffusion in single crystals, ultrathin films, and metal grown oxide structures

J. Carrasco
Departament de Quimica Fisica i Centre Especial de Recerca en Quimica Teorica, Universitat de Barcelona i Parc Cientific de Barcelona, C/Marti i Franques 1, 08028 Barcelona, Spain

N. Lopez
Institut Catala d'Investigacio Quimica, ICIQ, Universitat Rovira i Virgili, Avinguda dels Paisos Catalans 16, 43007 Tarragona, Spain

F. Illas[a)]
Departament de Quimica Fisica i Centre Especial de Recerca en Quimica Teorica, Universitat de Barcelona i Parc Cientific de Barcelona, C/Marti i Franques 1, 08028 Barcelona, Spain

H.-J. Freund
Fritz-Haber-Institut der Max-Planck-Gesselschaft, Faradayweg 4-6, 14195 Berlin, Germany

(Received 6 June 2006; accepted 13 July 2006; published online 21 August 2006)

The neutral oxygen vacancy (OV) energy formation for bulk, subsurface sites at different depths from the surface and various surface sites has been estimated for single crystals, unsupported ultrathin films of MgO, CaO, and BaO, and MgO ultrathin films supported on Ag(001). From the calculated energy barriers for diffusion through the surface and from the surface to the bulk it is found that diffusion is a hindered event, especially for MgO. Nevertheless, diffusion from the terrace to step edges is largely favored while diffusion through terrace sites is less likely and surface to bulk has a very low probability. It is argued that this explains recent scanning tunneling microscopy images for MgO thin films supported on Ag(001) showing OV populating preferentially the step edge sites. © *2006 American Institute of Physics*. [DOI: 10.1063/1.2335842]

I. INTRODUCTION

Metal oxides are essential in the search for new materials with applications in high temperature fuel cells, protective coatings, heterogeneous catalysis, and biocompatible materials.[1] The properties of oxides can be tuned by structuring the material—introducing steps and grain boundaries—by doping, or by removing some atoms from the structure—leading to compounds that deviate from the formal stoichiometry. Depending on the sample treatment, thermal heating or radiation, different kinds of oxygen vacancies (OVs) are created in the bulk and also at the surface.[2] These can be either electrically neutral, charged, or doubly charged; they can be paramagnetic and give rise to characteristic peaks in the electron paramagnetic resonance (EPR) spectra or be EPR silent.[3,4] Finally, O–O or Mg–O divacancies have also been proposed.[5,6] These point defects are known to have an important role on the catalytic activity of oxide surfaces.[3,7] For ultrathin MgO films grown on a given metal substrate[8] and on oxygen rich conditions the concentration of OVs is below detection limit. This is supported either from electron energy loss spectroscopy (EELS),[9] scanning tunneling microscopy (STM), and EPR.[10] OVs on these MgO thin films can be created by electron bombardment and their presence identified by the above mentioned experimental techniques.[9,10] However, STM images reveal that surface OVs thus created are mainly present at the edges and corners of the two dimensional finite islands grown on the metal template.[11]

For MgO single crystal, OV formation is an energetically costly process for both surface and bulk[12–14] and hence the experimentally found surface OV healing is not surprising.[9,10] Large formation energies have been also predicted for regular and low coordinated sites of other alkaline-earth oxide surfaces.[15] In the case of MgO, it has been shown that OV diffusion in the bulk[14] and through surface[16] is hindered by very large activation energy barriers. However, the information concerning OV formation and diffusion in supported ultrathin films is much scarcer.[17] OV formation energies and diffusion energy barriers for ultrathin films and single crystal models can be different because of the screening of the electrostatic potential by the underlying metallic substrate. To further understand the role of OV in the surface reactivity of single crystal and ultrathin film surfaces it is necessary to investigate the relative stability and mobility of OVs through the surface and also through the bulk.

In this work, we investigate OV stability and diffusion on models of MgO(001), CaO(001), and BaO(001) single crystals and silver grown MgO(001)/Ag(001) ultrathin films. The OV formation energy has also been studied as a function of the depth with respect to the surface, previous information being only available for MgO(001).[18] For the metal supported case, OV formation and diffusion involving regular surface and low coordinated step edge and kink sites have

[a)]Electronic mail: francesc.illas@ub.edu

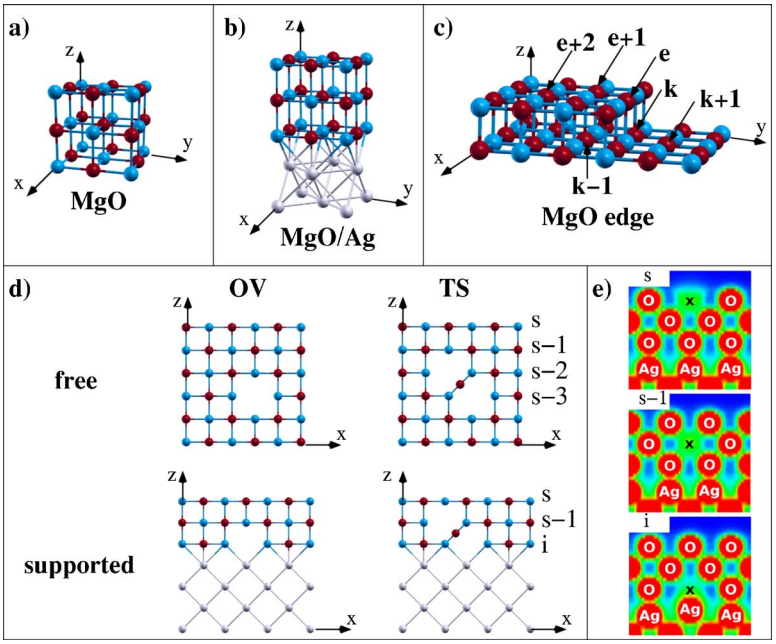

FIG. 1. (Color online) [(a) and (b)] Three dimensional model for the regular MgO and MgO/Ag structures. (c) Edge model sketch showing the different oxygen sites susceptible of OV formation positions. (d) Two dimensional simplistic sketches considering only z direction for equilibrium OV structures and transition states (TSs) showing the diffusion paths considered to deal with OV migration in alkaline-earth oxides (free and supported). (e) Electronic density at the vacancy site (marked as x) sitting at the surface (s), at the central layer ($s-1$), and at the interface (i) for a three-layer supported MgO film. Red (dark) spheres represent O atoms, blue (light) cations, and gray (quite light) stand for silver.

been also considered. Finally, to separate nano- and support effects on the MgO/Ag systems, we also investigate unsupported ultrathin slab limit. The main goal is to find out possible differences in these different MgO surface models due to nanosize, to OVs, different coordinations, or to the influence of the metal template.

II. COMPUTATIONAL DETAILS

We have performed first principles density functional (DF) calculations for different supercells of slabs representing single crystals and ultrathin films, see Fig. 1. Preliminary calculations including the usual tests of plane-wave cutoff, first Brillouin k-point sampling, as well as supercell size have been carried out to establish a converged and reliable numerical setup. Inner cores were described by the projector augmented-wave method[19] and the cut-off energy for the expansion of the monoelectronic valence states is 415 eV. The PW91 exchange-correlation potential[20] has been used together with a Monkhorst-Pack $2\times2\times1$ grid of k points. All DF calculations have been carried out with the VASP computational code.[21] We have restricted the study to neutral OVs because in a periodic approach charged defects will lead to unphysical interactions with the repeated unit cells. This could be avoided by adding a uniform background but this procedure may also introduce uncontrolled artifacts. Likewise, more complex defects such as O–O or Mg–O divacancies are not considered simply because the main goal of the present work is to study the various possible pathways for OV diffusion.

The MgO(001), CaO(001), and BaO(001) single crystal surfaces are represented by rather thick slabs of the cubic oxides cut along the (001) direction. The slab model for single crystal MgO(001) contains 12 atomic layers interleaved by a 12 Å vacuum width, whereas, because of the larger computational cost, the corresponding models for CaO(001) and BaO(001) single crystal surfaces contain 8 atomic layers. In all cases, the four bottom layers have been fixed to their bulk PW91-optimal positions (a_{MgO}=4.238 Å, a_{CaO}=4.843 Å, and a_{BaO}=5.610 Å) in the geometry optimization procedures. To simulate OV formation, a single O atom is removed from the $p(3\times3)$ supercell. In the case of unsupported ultrathin film slab models, two or three atomic layers and a somehow larger $3\sqrt{2}\times3\sqrt{2}$ surface supercell are considered. For the supported ultrathin films we have used the same slabs as in the unsupported models but placing the MgO atomic layers above a four-layered slab model for the Ag(001) surface. Consequently, the MgO unit cell is compressed by ~3% to match the Ag(001) lattice leading to a small tetragonal distortion of the MgO layers. Atomic positions in the upper two silver layers and entire oxide film have been allowed to relax, while the remaining atoms have been fixed in PW91-optimal, bulk Ag sites (a_{Ag}=4.160 Å). In order to simulate edged MgO supported ultrathin films a similar procedure has been chosen [see Fig. 1(c)]. Starting from a larger $p(4\times2)$ surface supercell with three oxide layers supported on three Ag atomic layers, keeping only fixed the last metal layer from the bottom of the slab; the corresponding edge has been generated by removing two consecutive MgO rows along the y direction from the outermost oxide layer. For the present set of oxides, the OV-OV interaction is small and for the concentrations employed here can be safely neglected.[14]

Since the symmetry of the systems almost remains upon OV formation, it is possible to approach the reaction path for diffusion by a constrained optimization thus enabling a considerable saving in computer time with respect to other means to locate transition state structures; especially for the very large supercells used to model the supported ultrathin films. Nevertheless, in almost all cases a full atomic relaxation of the atoms contained in the supercell, excluding the

TABLE I. OV formation energies (E^f, with respect to O ^3P) and diffusion barriers (E_a) in different configurations and layer positions for the given models used to approach several system types: MgO unsupported ultrathin films (containing 2 and 3 atomic layers), single crystal MgO(001) (approached by 12 atomic layers), and metal grown oxides containing both a MgO terrace and a MgO edge. For terrace models, the layers are denoted by $s-j$ as is depicted in Fig. 1(d), where s stands for the surface layer (first layer in the text) and j the level below the surface ($j=1$ for the second layer, $j=2$ for the third one, and so on). In the case of the edge model, the labels used to assign the different OV positions correspond to those given in Fig. 1(c). All energy values are in eV.

	Terrace models					Edge model	
	MgO			MgO/Ag			MgO/Ag
MgO layers	2	3	12	2	3		3
			E_f (eV)				
s	9.31	9.40	9.42	9.13	9.47	e	8.75
$s-1$	⋯	9.87	9.97	8.32	9.69	$e+1$	9.45
$s-2$	⋯	⋯	10.06	⋯	8.35	$e+2$	9.52
$s-3$	⋯	⋯	10.07	⋯	⋯	$k-1$	9.44
	⋯	⋯	⋯	⋯	⋯	k	9.54
	⋯	⋯	⋯	⋯	⋯	$k+1$	8.94
Bulk				10.08			
			E_a (eV)				
$s\leftrightarrow s$	2.41	2.60	2.69	1.55	2.13	$e\leftrightarrow(e+1)$	1.57/0.87
$s\leftrightarrow(s-1)$	2.59	3.11/2.65	3.42/2.87	1.23/2.04	2.70/2.40	$(e+1)\leftrightarrow(e+2)$	1.87/1.81
$(s-1)\leftrightarrow(s-2)$	⋯	⋯	3.93/3.84	⋯	1.24/2.58	$e\leftrightarrow k$	2.13/1.34
$(s-2)\leftrightarrow(s-3)$	⋯	⋯	4.14/4.13	⋯	⋯	$e\leftrightarrow(k-1)$	2.79/2.11
	⋯	⋯	⋯	⋯	⋯	$e\leftrightarrow(k+1)$	1.88/1.70
Bulk				4.21			

bottom slab layers as mentioned above, has accompanied the constrained search of the transition state (TS). This involves keeping partially fixed an oxygen atom halfway between two missing oxygen sites as found in the optimized regular system [Fig. 1(d)]. To search for alternative O-diffusing paths, the Cartesian coordinate perpendicular to the plane formed by the two missing centers and the O-diffusing atom (initially placed slightly out of the plane to avoid artificial symmetry constrains) has been allowed to relax during the optimization procedure. For specific cases where the diffusion process takes place near the metal-oxide interface, the atomic relaxation of all the atoms in the supercell was hindered. This is because large geometric rearrangements, which are noncompatible with any conceivable TS, are observed. In these cases, only the closer, yet sufficient large, neighbor region to the diffusing atom has been relaxed.

III. RESULTS AND DISCUSSION

A. Oxygen vacancy formation energies in MgO systems

The neutral vacancy formation energy, E^f, with respect to the O atom in the ^3P state depends on the position of the defect in the oxide slab (Table I). For a regular terrace site on a single crystal MgO(001) surface, E^f is 9.42 eV and becomes 10.06 eV at the third layer, value almost converged to the bulk one, which is 10.08 eV. The values predicted from periodic supercell DF calculations qualitatively agree with previous results for surface and subsurface obtained from Hartree-Fock[12] and DF hybrid functional[13] (B3LYP) calculations on embedded cluster models. Likewise, for subsurface OV formation, up to third layer below the surface, present DF calculations with the generalized gradient approximation (GGA) exchange-correlation potential are in agreement with previous estimates using the local density approach (LDA) carried out also on periodic models.[18] Consequently, OV formation at bulk and surface regular sites will not be further discussed.

Now, let us consider the case of unsupported ultrathin films containing two or three atomic layers. For these two-dimensional infinite systems, E^f is of 9.31 and 9.40 eV for the two- and three-layer models, respectively. For the three-layer slab, the E^f of an OV just beneath the surface is 9.87 eV or only 0.1 eV smaller than for the MgO single crystal. Hence, thickness, in the most extreme case, represents a reduction of ~0.1 eV (about a 1%) of the E^f. From these first values one can already conclude that OV formation energy is not largely affected by the reduced thickness on the direction perpendicular to the surface, in agreement with previous findings,[18] and provides additional support for the use of these thin films as valid models for single crystal oxide surfaces. Nevertheless, it is worth to point out that although previous LDA (Ref. 18) and present calculations agree in the rapid convergence of the E^f to the bulk, the former find a larger effect in going from the surface to deeper atomic layers, due to an overestimation of the bulk E^f magnitude compared with the same value computed in the present work.

A small effect of the slab thickness on the E^f values is

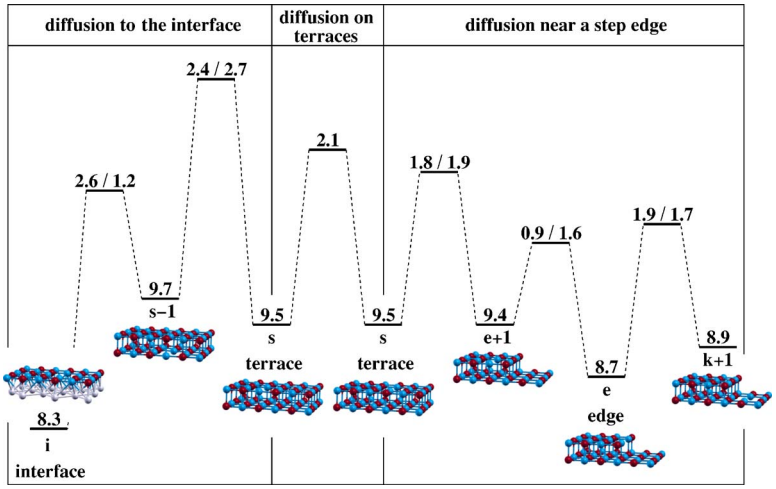

FIG. 2. Energy profile (in eV) for the diffusion of oxygen vacancies of MgO (three atomic layers) thin films supported on Ag(001); both OV E^f and E_a are presented. The central panel corresponds to diffusion between surface terrace sites, the left panel shows the profile for diffusion from terrace sites to the inner layers and to the interface, and the right panel stands for the diffusion from terrace sites to the step edge and underlying terrace sites (see Fig. 1). Structural models representative of the various vacancy configurations considered are given in the insets.

also found for the MgO ultrathin films supported on Ag(001). However, in this case, the presence of the underlying metal substrate has a non-negligible role, as already pointed out by Lopez and Valeri.[17] For the MgO/Ag supported ultrathin films, terrace OV formation energy becomes 9.13 and 9.47 eV for the slab models containing two or three atomic layers, respectively. For the three-layer metal supported film, this is almost the same than for the unsupported material. Hence, the influence of the support is small and noticeable for the two-layer film only. In the case of supported ultrathin films a different situation arises which corresponds to OV formation at the metal-insulator interface. For the interface OVs we find $E^f \sim 8.3$ eV, which implies an important reduction ($\sim 10\%$) with respect to the surface case either for the two-or three-layer films; it is even lower than the OV formation energy on low coordinated sites corresponding to the step edge model (8.75 eV). This low value for the predicted formation energy of OV at the metal-oxide interface is the consequence of a partial charge transfer from the oxide to the metal as indicated by the density plots on Fig. 1(e) and already identified by Giordano *et al.*[22] Indeed, it has been argued that interface OVs are needed to stabilize the oxide film above the metal surface.[17]

B. Oxygen vacancy diffusion energy barriers in MgO systems

A complete description of the OV containing oxide surfaces requires also the activation energies for OV diffusion either through the surface or between the surface and the bulk. A complete set of values for the different MgO and MgO/Ag systems considered in this work is also given in Table I. For a MgO single crystal, diffusion through terrace sites costs 2.69 eV, in excellent agreement with previous LDA calculations,[16] whereas diffusion from the surface to the subsequent layers in the film involves larger energy barriers of 3.42, 3.93, and 4.13 eV converging to 4.21 eV for bulk diffusion. Experimentally, a broad range of OV bulk diffusion barrier estimates exists, essentially due to the difficulty to accurately measure this magnitude arising from the fact that, under experimental conditions, F center diffusion competes with other processes also taking place upon sample annealing.[23,24] Indeed, experimental values for energy barriers smaller than 3.4 eV have been argued to be related to these competing processes.[23] Notice that the surface to subsurface energy barrier for MgO predicted in the present work is 3.4 eV, similar to the experimental estimate obtained from the decay of the optical fingerprint corresponding to the surface OV center.[23,25] The difference between the energy barriers described above is large enough to conclude that whenever OVs exist at the surface, OV transport within the surface will occur at lower temperatures and will always prevail while OVs in deeper layers on the material will tend to be more static. For unsupported thin films the situation remains almost the same as expected from the discussion above. In fact, the values for the three-layer slab are 2.60 and 3.11 eV, respectively (2.65 eV for the diffusion from the second layer to the surface). For the two-layer ultrathin film the barriers for diffusion through the surface and through the film are close to each other but the former (2.41 eV) is still smaller than the latter (2.59 eV). Notice that barriers for diffusion from the surface to subsurface layer in the single crystal and on the three-layer film differ by less than 0.3 eV, indicating a very fast convergence of this property with the film thickness. Therefore, one can conclude that OV diffusion in single crystal and unsupported thin films will be very similar with noticeable differences for the extreme case of two atomic layer slabs only.

For the supported ultrathin films the situation is very similar except for the case containing just two atomic layers, which represents a limiting case. In fact, for this extremely thin slab, diffusion to the interface is favored with respect to diffusion through the surface. For the OVs at edges it is interesting to point out that the most favorable process involves diffusion from the terrace to the edge [$e+1 \rightarrow e$ in Fig. 1(c)] with an energy barrier of 0.87 eV, which is much smaller than the barriers reported above for diffusion either through the terrace or through the bulk (Fig. 2). Once the OVs reach an edge site they are trapped, since the inverse process implies an energy barrier of 1.57 eV. The rest of the possible competing diffusion processes all have larger energy barriers, the lowest one involves diffusion from the edge to a site of the underlying terrace [$e \rightarrow k+1$ in Fig. 1(c)], but the corresponding energy barrier is 1.88 eV. To conclude, OV diffusion from the surface to the bulk is a highly unlikely

TABLE II. OV formation energies (E^f) with respect to O ^3P and diffusion barriers, E_a; for different layer positions for CaO and BaO unsupported ultrathin films (two and three atomic layers) and single crystal (eight atomic layers). All energies are in eV.

		E^f (eV)				
	No. of layers	s	$s-1$	$s-2$	$s-3$	Bulk
CaO	2	9.09				10.14
	3	9.26	9.80			
	8	9.26	9.93	10.07	10.10	
BaO	2	9.94				9.05
	3	8.13	8.54			
	8	8.26	8.79	9.01	9.05	
		E_a (eV)				
	No. of layers	$s\leftrightarrow s$	$s\leftrightarrow(s-1)$	$(s-1)\leftrightarrow(s-2)$	$(s-2)\leftrightarrow(s-3)$	Bulk
CaO	2	2.11	1.77/1.77			3.44
	3	2.02	2.54/1.99			
	8	2.08	2.78/2.11	3.18/3.04	3.31/3.28	
BaO	2	0.95	0.79/0.79			1.42
	3	0.38[a]	1.08/0.67			
	8	0.61	1.31/0.77	1.57/1.36	1.49/1.45	

[a]The small energy barrier found arises from the different transition state structure observed when compared to three-layer CaO and MgO slabs.

process but diffusion through the surface terraces is less energy costly and diffusion to step edge sites involves even smaller energy barriers. Consequently, once the OVs reach the step edge sites they are trapped since further diffusion is hindered by much larger energy barriers. However, notice that the smallest energy barrier involves diffusion from a terrace site nearest to a step edge site towards a step edge site $(e+1\rightarrow e)$, 0.87 eV; but the energy barrier for OVs to diffuse from one terrace site to another $(e+1\rightarrow e+2)$ is of the order of the energy barriers for diffusion from the step edge to the nearest terrace sites $(e\rightarrow e+1)$. Consequently, in case the temperature is large enough to permit the diffusion through surface sites, the trapping at step edge sites will have a dynamic character.

C. Oxygen vacancy formation and diffusion in other simple oxides

In order to have a more complete picture of the OV formation and diffusion on these simple oxides we considered the case of two, three, and eight atomic layers of CaO and BaO. CaO is very similar to MgO, whereas BaO is less ionic.[26] The OV formation energy (Table II) follows the trend already discussed for MgO. For both, CaO and BaO, OV formation is always easier in the surface. The present results from periodic DF calculations are in good agreement with recent results reported by Di Valentin *et al.*[15] using a hybrid exchange functional (B3LYP) and finite embedded cluster models. For OV formation below the surface, present calculations show that for CaO and BaO E^f values also converge rapidly towards the bulk value, stable values being already achieved at the third atomic layer below the surface.

In a similar way, the diffusion through the surfaces is always favored with respect to diffusion through the bulk with the only obvious exception of the two-layer models (Table II). Therefore, for realistic models of CaO and BaO, OV diffusion through the surface will also dominate with respect to diffusion to the bulk. An important difference with respect to MgO concerns the absolute magnitude of the OV diffusion energy barriers. In fact, the OV diffusion energy barriers for CaO and BaO are significantly smaller than those corresponding to MgO; especially for BaO. Hence, one may predict that OV diffusion in BaO can start near room temperature. The reduction of the corresponding diffusion energy barriers along the alkaline-earth series can be explained by the concomitant decrease of the Madelung potential when moving down along the series[14] and the more open lattice structures. In fact, important changes in the structure of the transition states between the different oxides are observed, especially for the diffusion through the surface. For the TS corresponding to MgO(001) surface OV diffusion, the diffusing oxygen atom is placed ~0.10 Å above the surface plane, whereas for CaO(001) and BaO(001) the diffusion path is subsurface with a TS structure having the O-diffusing atom at ~0.77 and ~1.00 Å below the surface plane, for CaO(001) and BaO(001), respectively. At first sight this may seem a quite strange path but it is fully confirmed by the calculation of a section of the potential energy surface on a sufficiently dense grid. The results indicate the presence of two different TS structures, one above and another below the surface plane. In the case of the MgO(001) surface the former is the lowest energy TS, whereas in the case of CaO(001) and BaO(001) the lowest energetic TS corresponds to that one where the O atom diffuses below the surface.

IV. CONCLUSIONS

The conclusions emerging from the results discussed in the preceding section above can be summarized as follows.

(1) OV formation energies are large but they decrease along the alkaline-earth series and in going from bulk to the surface and from surface regular sites to the low coordinated ones, in agreement with previous findings using embedded cluster models.[12,15] Likewise, for the whole series, OV formation energies for subsurface sites converge rapidly towards the bulk, in agreement with previous results for MgO.[18]

(2) OV diffusion through the surface is always preferred with respect to diffusion through the bulk and it is particularly preferred for diffusion towards step edges which become OV dynamic traps. Nevertheless, the calculated OV diffusion barriers are rather large indicating that this is an unlikely process except for BaO or under annealing conditions.

The present results are in full agreement with recent observations indicating that (i) OVs are rather uncommon for both single crystal and thin films supported on a metal template and only present after being produced through aggressive treatments such as heating, ion bombardment, and cleaving[10] and (ii) OVs tend to aggregate at the step edges.[11] In fact, once OVs are formed diffusion either through the surface or through the bulk becomes possible at high temperatures—the former process being largely dominant—with diffusion to step edge sites being preferred over other possible diffusion paths. This is a clear consequence of the relative values for OV diffusion reported in Tables I and II.

ACKNOWLEDGMENTS

One of the authors (J.C.) thanks MEC for predoctoral grant and another author (N.L.) thanks the ICIQ Foundation. Financial support comes from DGICYT (BQU2002-04029-CO2-01 and UNBA05-33-001), GenCat (2005SGR-00697 and 2005 PEIR 0051/69), and DGCPRU [to two of the authors (F.I. and N.L.)]. The CEPBA-IBM is acknowledged for computer time allocation.

[1] V. E. Henrich and P. A. Cox, *The Surface Science of Metal Oxides* (Cambridge University Press, Cambridge, 1994).
[2] *The Chemical Physics of Solid Surfaces: Oxide Surfaces*, edited by P. Woodruff (Elsevier, Amsterdam, 2001), Vol. 9.
[3] G. Pacchioni, ChemPhysChem **4**, 1041 (2003).
[4] D. M. Murphy, R. D. Farley, I. J. Purnell, C. Rowlands, A. R. Yacob, M. C. Paganini, and E. Giamello, J. Phys. Chem. B **103**, 1944 (1999).
[5] D. Dominguez-Ariz, C. Sousa, F. Illas, D. Ricci, and G. Pacchioni, Phys. Rev. B **68**, 054101 (2003).
[6] D. Ricci, G. Pacchioni, P. V. Sushko, and A. L. Shluger, J. Chem. Phys. **117**, 2844 (2002).
[7] E. Wahlström, N. Lopez, R. Schaub, P. Thostrup, A. Rønnau, C. Africh, E. Lægsgaard, J. K. Nørskov, and F. Besenbacher, Phys. Rev. Lett. **90**, 026101 (2003).
[8] H.-J. Freund, Angew. Chem., Int. Ed. Engl. **36**, 452 (1997).
[9] J. Kramer, W. Ernst, C. Tegenkamp, and H. Pfnür, Surf. Sci. **517**, 87 (2002); J. Kramer, C. Tegenkamp, and H. Pfnür, Phys. Rev. B **67**, 235401 (2003).
[10] M. Sterrer, E. Fischbach, T. Risse, and H.-J. Freund, Phys. Rev. Lett. **94**, 186101 (2006).
[11] M. Sterrer, M. Heyde, M. Novicki, N. Nilius, T. Risse, H.-P. Rust, G. Pacchioni, and H.-J. Freund, J. Phys. Chem. B **110**, 46 (2006).
[12] P. Pescarmona and G. Pacchioni, Surf. Sci. **412/413**, 657 (1998).
[13] P. V. Sushko, A. L. Shluger, and C. R. A. Catlow, Surf. Sci. **450**, 153 (2000).
[14] J. Carrasco, N. Lopez, and F. Illas, Phys. Rev. Lett. **93**, 225502 (2004).
[15] C. Di Valentin, R. Ferullo, R. Binda, and G. Pacchioni, Surf. Sci. **600**, 1147 (2006).
[16] F. Finocchi, J. Goniakowski, and C. Noguera, Phys. Rev. B **59**, 5178 (1999).
[17] N. Lopez and S. Valeri, Phys. Rev. B **70**, 125428 (2004).
[18] L. N. Kantorovich, J. M. Holender, and M. J. Gillan, Surf. Sci. **343**, 221 (1995).
[19] G. Kresse and D. Joubert, Phys. Rev. B **59**, 1758 (1999).
[20] J. P. Perdew, J. A. Chevary, S. H. Vosko, K. A. Jackson, M. R. Pederson, D. J. Singh, and C. Fiolhais, Phys. Rev. B **46**, 6671 (1992); J. A. White and D. M. Bird, *ibid.* **50**, 4954 (1994).
[21] G. Kresse and J. Hafner, Phys. Rev. B **47**, 558 (1993); G. Kresse and J. Furthmüller, *ibid.* **54**, 11169 (1996).
[22] L. Giordano, J. Goniakowski, and G. Pacchioni, Phys. Rev. B **67**, 045410 (2003).
[23] A. I. Popov, M. A. Monge, R. González, Y. Chen, and E. Kotomin, Solid State Commun. **118**, 163 (2001).
[24] A. De Vita, M. J. Gillan, J. S. Lin, M. C. Payne, I. Stich, and L. J. Clarke, Phys. Rev. B **46**, 12964 (1992).
[25] V. N. Kuzovkov, A. I. Popov, E. A. Kotomin, M. A. Monge, R. González, and Y. Chen, Phys. Rev. B **64**, 064102 (2001).
[26] G. Pacchioni, C. Sousa, F. Illas, F. Parmigiani, and P. S. Bagus, Phys. Rev. B **48**, 11573 (1993).